

Modeling the Rate of Cadmium and Selenite Adsorption on Micro- and Mesoporous Transition Aluminas

CHARALAMBOS PAPELIS,*†
PAUL V. ROBERTS, AND
JAMES O. LECKIE

*Environmental Engineering and Science,
Department of Civil Engineering, Stanford University,
Stanford, California 94305-4020*

The rates of cadmium and selenite uptake by porous aluminas were studied using three porous transition aluminas. The three adsorbents differed in size and pore structure, CP-5 and CP-100 being the smallest and largest particles, respectively, both exhibiting some microporosity, and C-33 being intermediate-size, mesoporous particles. The rate data were interpreted with a diffusion model, assuming solute diffusion in a sphere from limited volume. The diffusion model was in fair agreement with the rate data, suggesting that cadmium and selenite uptake is controlled by intraparticle mass transfer. Solute uptake by the smaller particles (CP-5) was considerably faster than uptake by the larger particles (CP-100). The measured apparent diffusivities for both adsorbates and all adsorbents were orders of magnitude lower than bulk aqueous diffusivities, in accordance with expectations for highly retarded sorption. The measured effective diffusivities were substantially lower than aqueous molecular diffusivities, suggesting the presence of strong hindrance effects in these microporous adsorbents.

Introduction

Fate and transport of hazardous chemicals in the environment largely depend on the interaction of these substances with mineral phases in soils and aquifers. A number of transport models attempt to incorporate these interactions by using an equilibrium distribution coefficient, K_d , describing the partitioning of a substance at the solid-solution interface. As was pointed out, however (1-6), equilibrium distribution coefficients may not adequately describe the partitioning of an organic chemical at the solid-solution interface because of sorption rate limitations. It is believed that intraparticle mass transfer is responsible for the observed slow uptake of organic contaminants by aquifer material (1).

Inorganic ion fate and transport have received considerable attention because of the implications for radionuclide migration in subsurface environments. The kinetics of inorganic ion sorption on mineral surfaces are not well understood, partly because of the complex processes occurring at mineral-water interfaces. In the late 1940s, research associated with the Plutonium Project focused on the rate of ion exchange of alkali metals on synthetic organic zeolites (7, 8). They concluded that the rate of ion exchange was determined either by internal diffusion or by external liquid film resistance. Similarly Ogwada and Sparks (9, 10) more recently recognized the effect of mass transfer on ion exchange kinetics in clay minerals. In the majority of studies of inorganic ion rate of uptake by oxides, however, a distinct two-step behavior is reported, including a fast initial uptake followed by much slower gradual uptake that may continue for a period of days to months (11-13).

Several mechanisms have been postulated to explain this slow uptake, including formation of binuclear complexes, particle-particle interactions, diffusion into adsorbents, and surface precipitation (11). In most cases the slow uptake step was interpreted in terms of intrinsic chemical reaction rates (mass transfer independent) (14, 15), which in the case of strongly-binding, inner-sphere complex-forming ions could be explained by the slow rate of hydration water loss, a necessary step in the formation of inner-sphere, surface coordination complexes (16). Pressure jump studies, however, have shown that ion attachment on mineral surfaces is very fast for a variety of anions, cations, and mineral surfaces (17-23). Pressure jump techniques, using nonporous mineral surfaces, can eliminate mass transfer limitations and measure intrinsic rates of fast sorption reactions. A surface precipitation model (24) was invoked to account for the slow uptake of cadmium by ferrihydrite at high sorbate/sorbent ratios (25), whereas diffusion inside ferrihydrite aggregates was invoked to explain the slow uptake of arsenate by ferrihydrite (26).

An additional difficulty in modeling the fate and transport of inorganic pollutants in subsurface environments stems from the use/misuse of the conditional equilibrium distribution coefficient, K_d . The distribution coefficient concept has been used extensively to model

* To whom all correspondence should be addressed.

† Present address: Desert Research Institute, Water Resources Center, University System of Nevada, P.O. Box 19040, Las Vegas, Nevada 89132-0040; e-mail address: jambis@snsr.unr.edu.

partitioning of both organic and inorganic solutes onto sediments and mineral surfaces. For organic solute partitioning on mineral surfaces, K_d is a function of the sorbate and sorbent, but it generally correlates with the organic fraction of the mineral phase (27). For inorganic solute sorption on mineral surfaces, K_d is a strong function of pH, temperature, and other geochemical conditions (e.g., speciation and redox potential) (16).

Use of the distribution coefficient to model solute partitioning assumes that the sorption isotherm is essentially linear over the concentration range of interest. Use of K_d values to model ion sorption on mineral surfaces without reference to specific experimental conditions can lead to gross errors in sorption behavior predictions (28). It was pointed out that the use of distribution coefficients to predict the fate and transport of inorganic contaminants in natural hydrogeological environments requires estimation of the distribution coefficients under, if possible, identical geochemical conditions to those found in the site being studied. Failure to do so may result in severe underestimation of the zone of contamination and the time required for contaminated aquifer rejuvenation (29).

Unfortunately, the use of distribution coefficients without explicit reference to the specific experimental conditions used to derive these coefficients is still fairly common in radionuclide transport models (30–32). Use of equilibrium distribution coefficients is warranted only if the conditions (including pH) are maintained constant during the experiment and the equilibrium coefficients are determined under the same experimental conditions, as was done in this study. A more rigorous, but substantially more involved, approach to the use of distribution coefficients is the use of surface complexation models (33).

To test the hypothesis that the rate of cadmium and selenite uptake in porous particles is controlled by intraparticle diffusion, time-dependent sorption experiments were conducted with porous alumina particles having different particle size (CP-5 and CP-100) but otherwise similar characteristics. Particles with larger dimensions (length of diffusion path) were expected to require longer equilibration times if the rate was controlled by intraparticle diffusion. To evaluate effects of crystal and pore structure on trace element uptake, a third transition alumina (C-33) with a higher degree of crystallinity and wider pores was also used.

Although the adsorbents used in this study are not expected to be found in nature (see the following section for a brief adsorbent characterization), transport of inorganic ions in aquifers can be controlled by intraparticle diffusion in minerals exhibiting intraparticle porosity, such as natural zeolites and the disordered aluminosilicate minerals collectively referred to as allophane and imogolite. In addition, contaminant sorption on porous iron coatings and in the interlayer spacings of smectite clays can be controlled by intraparticle mass transfer. Transport of Li^+ in a sandy aquifer was significantly affected by intragranular porosity of sand-size sediments (34). Because of the abundance of aluminol sorption sites in nature (as part of aluminosilicate minerals), being able to distinguish between kinetically and mass transfer limited rate of ion uptake by these oxides is important for our understanding of factors affecting the transport of contaminants in aquifers. In addition, large porous oxides with high internal surface area could be used as trace element adsorbents in engi-

neering applications, but the rate of sorption could be severely limited by intraparticle diffusion.

The distribution coefficients, used for the analysis of the rate data presented here, were estimated from sorption experiments with 1 week equilibration time. It was shown from preliminary experiments that longer equilibration times resulted in fractional uptake changes within the uncertainty of the measurements. Very slow processes, including solid diffusion and the potential transformation of the transition aluminas used in this study (which are thermodynamically not stable under ambient conditions), were obviously not allowed to reach equilibrium. True equilibrium (in a thermodynamic sense) therefore was probably not reached within the week-long equilibration time. The conclusions presented here, however, which are based on the assumption that equilibrium was reached within 1 week, are still valid, based on the much shorter time scale of diffusion and sorption processes compared to solid solution formation and phase transformation processes.

Materials and Methods

All three adsorbents were transition aluminas, products of the thermal transformation of aluminum hydroxides (or oxyhydroxides) to corundum ($\alpha\text{-Al}_2\text{O}_3$). CP-5 and CP-100 were more disordered, low-temperature forms, exhibiting some microporosity, whereas C-33 was a more crystalline, high-temperature form, exhibiting no microporosity. Pores with diameters larger than 500 Å (50 nm), between 500 and 20 Å (50–2 nm), and smaller than 20 Å (2 nm) are classified as macro-, meso-, and micropores, respectively (35). Approximately 50% of the BET surface area of CP-5 and CP-100 was associated with micropores, whereas the entire BET surface area of C-33 was associated with mesopores. A summary of particle characteristics relevant to this paper is given in Table 1. The complete physicochemical characterization of the adsorbents, including scanning and transmission electron micrographs and surface area distribution as a function of pore diameter, was presented elsewhere (36).

All experiments were conducted in 0.01 M sodium nitrate at 25 °C. Overhead Talboys stirrers were used for mixing to avoid particle abrasion and size reduction. Particle size distribution and surface area measurements, performed before and after the experiments, suggest that the experiments did not affect particle characteristics. Impeller speed was adjusted to keep the particles in suspension. Slurry samples from different depths did not indicate any significant variations in particle size distribution as a function of depth. The pH was maintained constant throughout the experiment by the addition of sodium hydroxide or nitric acid.

The experimental procedures were as follows. The solid was equilibrated with Milli-Q water in 35 mL polypropylene centrifuge tubes for at least 24 h. The slurry was transferred to a 500-mL jacketed reactor and equilibrated with the electrolyte for an additional 24 h. The pH was adjusted with sodium hydroxide or nitric acid to the desired pH value for the experiment. The pH at which uptake experiments were conducted was chosen based on equilibrium experiments so that fractional uptake at equilibrium was between 40 and 90%. After equilibration of the slurry at the desired pH, adsorbate addition (including a radioactive tracer) to the reactor marked the beginning of the experiment. Samples were withdrawn as a function of time

TABLE 1

Summary of Particle Characteristics

	CP-5	C-33	CP-100
	Particle Diameters (μm)		
mass mean diameter (d_w)	9.1	41.5	73.3
volume surface mean (Sauter mean diameter)	8.3	34.0	58.0
	Surface Area (m^2/g) and Porosity		
N_2 -BET	200	110	170
micropore volume ($\text{cm}^3(\text{STP})/\text{g}$)	24	0	20
porosity (-)	0.75	0.74	0.66
typical pore diameters (\AA)	< 20	20-100	< 20
	Surface Stoichiometry/Crystal Structure		
$\text{Al}_2\text{O}_3 \cdot x\text{H}_2\text{O}$; $x =$	0.5	0.1	0.8
crystal structure	disordered, low-temp. transition alumina	poorly cryst., high-temp. transition alumina	disordered, low-temp. transition alumina

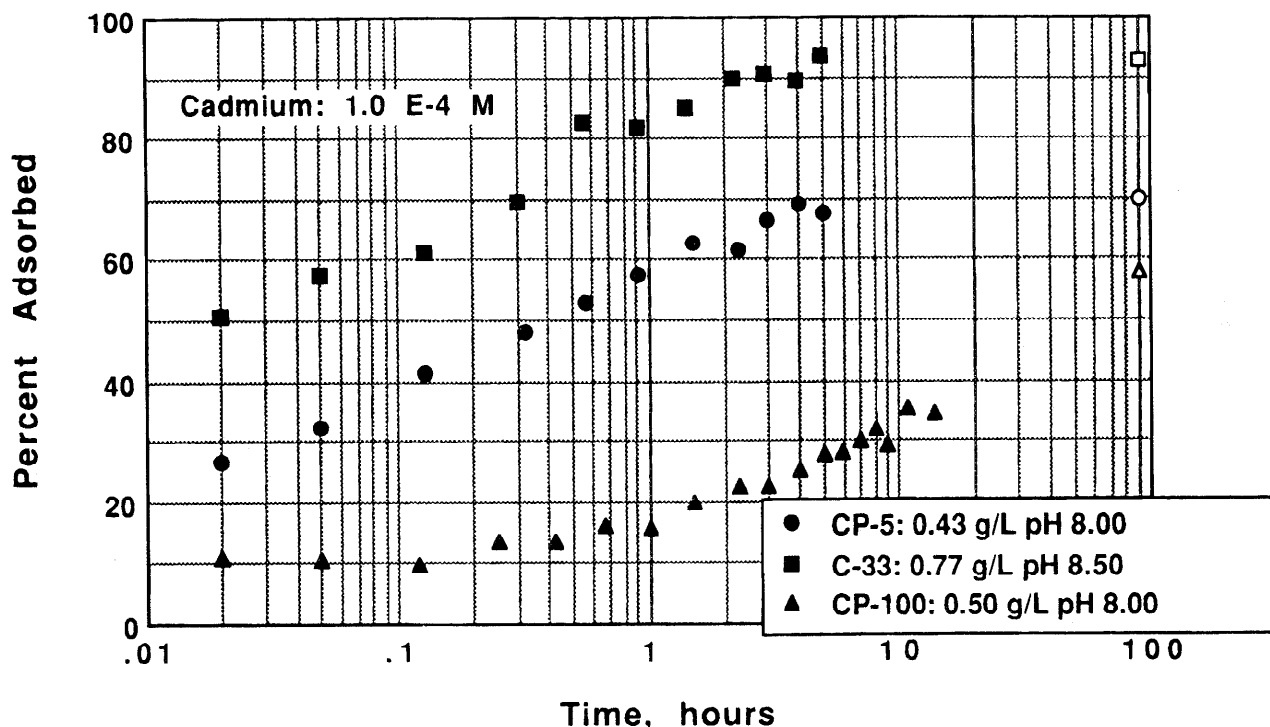


FIGURE 1. Rate of cadmium uptake by transition aluminas (CP-5, C-33, and CP-100) in 0.01 M NaNO_3 . Filled symbols correspond to rate data (at specified solid concentration and pH); open symbols correspond to equilibrium sorption under the same conditions.

with a 20-mL plastic syringe equipped with a three-way stopcock to which a Teflon tube (for sampling) and a 0.2- μm nylon filter (Alltech Nylon 66, 25 mm) were attached. The slurry was immediately filtered (total sampling time was less than 1 min), and fractional uptake was determined by comparing the radioactivity in the filtrate to the total radioactivity in the slurry. Sampling was more frequent in the earlier stages of the experiment when the rate of change was greatest. pH variation during the course of the experiment did not exceed 0.02 unit.

Results and Discussion

Results of uptake rate experiments are reported for cadmium and selenite in Figures 1 and 2, respectively. The rate data (filled symbols) are presented as fractional uptake versus time (log scale); the fractional uptake values corresponding to the equilibrium isotherms (Appendix) are shown as open symbols.

Cadmium. Experiments were conducted at a range of adsorbent/adsorbate ratios and different pH values. Some

characteristic rate of uptake experiments with cadmium and the transition aluminas are shown in Figure 1. The fractional cadmium uptakes by the three transition aluminas (CP-5, C-33, and CP-100) are shown as a function of time. It should be noted that the final uptake of cadmium (at equilibrium) for the experiments shown was not 100%. To facilitate data analysis, both cadmium and selenite uptake experiments (Figures 1 and 2) were designed so that the final uptake (at equilibrium) would be between 40 and 90%. The initial cadmium concentration was 1.0×10^{-4} M. Solid concentrations were adjusted so that the total BET surface area would be the same for the three adsorbents.

Several observations can be made by inspection of Figure 1. By comparing uptake by the CP-5 and CP-100 oxides, we see that approximately 40% of total cadmium uptake (at equilibrium) was achieved within the first minute of the experiment in the case of CP-5 particles; uptake by CP-100 particles proceeded more slowly, and the initial (instantaneous) sorption was significantly reduced. Adsorption

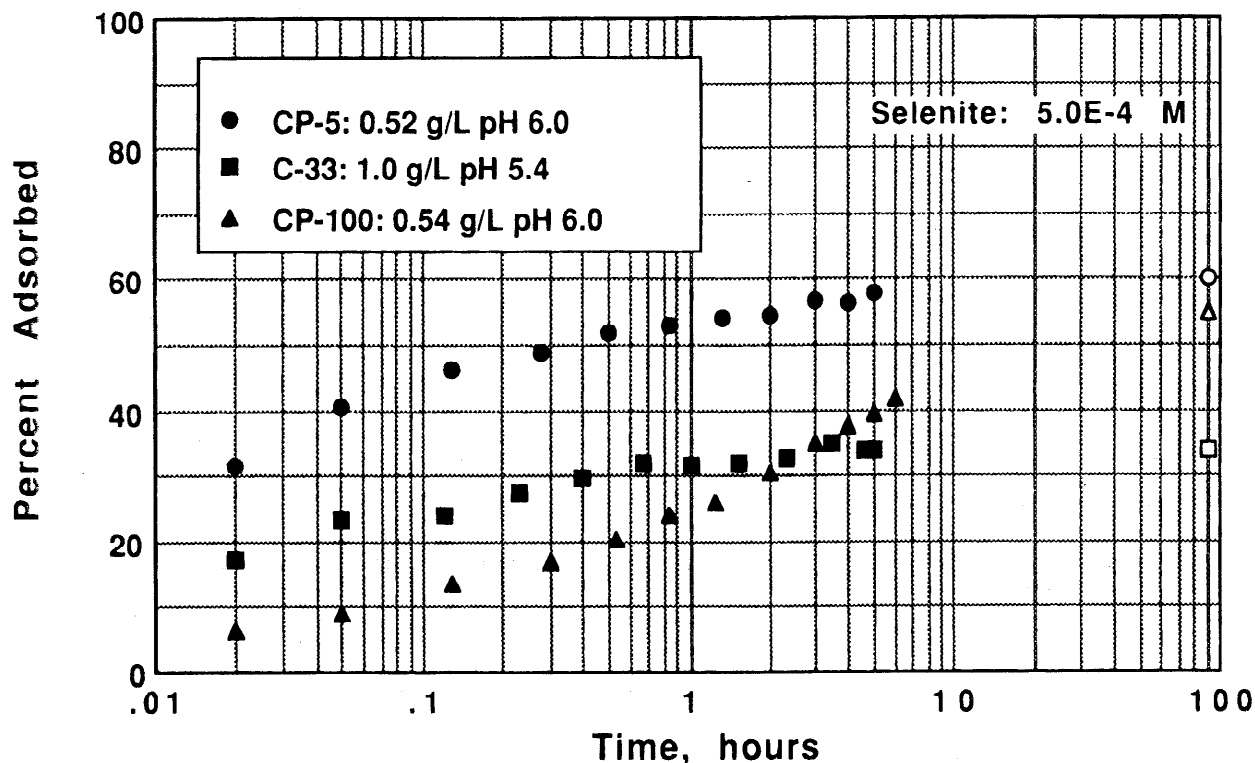


FIGURE 2. Rate of selenite uptake by transition aluminas (CP-5, C-33, and CP-100) in 0.01 M NaNO_3 . Filled symbols correspond to rate data (at specified solid concentration and pH); open symbols correspond to equilibrium sorption under the same conditions.

on CP-5 particles appeared to reach equilibrium after approximately 3 h, whereas adsorption on CP-100 particles continued to increase substantially even after 10 h. Equilibrium was not reached for the CP-100 particles until after several days; final equilibrium uptake, however, was similar for CP-5 and CP-100 adsorbents as shown by the K_d values in Table 4 (36).

The CP-5 and CP-100 adsorbents had similar characteristics, except for particle size (36), as shown in Table 1. The larger sized CP-100 particles sorbed cadmium considerably more slowly, requiring approximately 100 times as long to reach a given percent adsorbed. The uptake experiments thus support the hypothesis that the rate of cadmium uptake is controlled by mass transfer, specifically intraparticle diffusion. A comparison of external (film) and internal (intraparticle) mass transfer resistance indicates that it is rather unlikely that external mass transfer could affect the observed rate of uptake, based on a calculated ratio of internal to external mass transfer resistance between 100 and 1600, depending on adsorbate and adsorbent (36).

In the case of the smaller CP-5 particles, a significant fraction of the total surface area is located within a short distance from the external surface of the particle and is therefore easily accessible. Rapid access to a substantial fraction of the surface area explains the fast initial uptake of cadmium by CP-5. In the CP-100 particles, the diffusion path is substantially longer than in CP-5, and a smaller fraction of the total surface area is quickly accessible, explaining the smaller fraction of instantaneous sorption and slower uptake. The fast initial uptake by CP-5 suggests that the intrinsic, mass transfer independent, chemical reaction is fast, in agreement with previous studies of intrinsic adsorption rates (17, 18, 20).

Cadmium uptake by C-33 followed a pattern similar to uptake by CP-5, even though C-33 particles were larger than CP-5 (Table 1). The differences (and similarities) in

behavior between the three adsorbents can be explained by their structural differences. Both CP-5 and CP-100 were disordered, low-temperature transition aluminas, with similar pore dimensions and partly microporous, whereas C-33 was a more crystalline, high-temperature transition alumina, exhibiting no microporosity. Approximately 50% of the total BET surface area was associated with micropores in the CP-5 and CP-100 particles, whereas the entire surface area was associated with macro- and mesopores in C-33 particles. Pore diameters smaller than 20 Å were definitely present in CP-5 and CP-100 particles, as suggested by nitrogen sorption experiments, and have been reported in the literature (37). It is very difficult, however, to estimate the lower end of pore diameters in these particles. The mesoporous particles, C-33, had pore diameters primarily between 20 and 100 Å (Table 1).

Essentially the only difference between CP-5 and CP-100 particles was their size (Table 1). The latter accounts for the difference in rates of solute uptake between CP-5 and CP-100 particles. The wider pore structure, absence of microporosity, and higher crystallinity of the C-33 particles could probably explain the relatively faster solute uptake by C-33 compared to CP-5 particles. (Equilibrium was reached within 2–3 h for both CP-5 and C-33 particles, even though the diffusion path was longer in the C-33 particles.)

Selenite. Characteristic selenite uptake rate experiments are shown in Figure 2. The initial selenite concentration in the experiments shown was 5.0×10^{-4} M. The solid concentrations and pH were varied to account for differences in specific surface areas and selenite binding affinities of the three solids. The experiments were conducted at or below pH 6 to maximize uptake for a given sorbate/sorbent ratio and to minimize the effects of slight pH fluctuations during the course of the experiments (a steeper adsorption "edge" is equivalent to increased uptake sensitivity as a

TABLE 2

Cadmium Diffusivities in Porous Aluminas^a

	CP-5	C-33	CP-100
K_d (m ³ /g)	1.0×10^{-2}	1.1×10^{-2}	1.1×10^{-2}
R_{int} (-)	1.0×10^4	1.3×10^4	1.6×10^4
pH	8.0	8.5	8.0
D_{app} (m ² /s)	4.0×10^{-16}	1.0×10^{-15}	4.0×10^{-16}
D_{eff} (m ² /s)	4.1×10^{-12}	1.3×10^{-11}	6.3×10^{-12}
χ_e (-)	300	95	200

^a $D_{mol} = 1.23 \times 10^{-9}$ m²/s.

function of pH). The solid concentrations were 0.52, 1.0, and 0.54 g/L for CP-5, C-33, and CP-100, respectively.

The general trends for cadmium and selenite uptake were similar. Selenite uptake by CP-5 and C-33 was fast compared to uptake by CP-100. Equilibrium was reached within 1–3 h in the case of CP-5 and C-33 particles; in the case of CP-100 particles, uptake continued to increase even after 7 h. These data in combination with equilibrium adsorption experiments suggest that for CP-100 particles equilibrium required several days. Similar to cadmium uptake, selenite uptake by C-33 was faster than expected from size considerations alone; the fast uptake can be explained by the mesoporous structure of the solid.

Modeling Approach. The rate of cadmium and selenite uptake by porous aluminas was modeled assuming diffusion of solute in a sphere from a well-stirred reactor of limited volume and fixed initial solute concentration. The analytical solution of the diffusion equation (eq 1) is given by Crank (38):

$$\frac{\partial C}{\partial t} = D_{app} \frac{\partial^2 C}{\partial x^2} \quad (1)$$

where $C = 0$ at $t = 0$ for $x < a$; $C = C_o$ at $t = 0$ for $x > a$; a is the sphere radius; and

$$D_{app} = \frac{D_{mol}}{\chi \left(1 + \frac{\rho_b K_d}{\epsilon} \right)} \quad (2)$$

$$D_{eff} = \frac{D_{mol}}{\chi} = D_{app} \left(1 + \frac{\rho_b K_d}{\epsilon} \right) \quad (3)$$

and

$$R_{int} = 1 + \frac{\rho_b K_d}{\epsilon} \quad (4)$$

D_{app} is the apparent diffusivity (m²/s); D_{eff} is the effective diffusivity (m²/s); D_{mol} is the molecular diffusivity (m²/s); χ is the tortuosity (-); ρ_b is the solid bulk density (kg/m³); R_{int} is the internal retardation factor (-); K_d is the conditional distribution coefficient (m³/kg); ϵ is the porosity. The model requires specification of the initial solute concentration in the reactor at time $t = 0$, C_o , and the final solute concentration at equilibrium, C_∞ . The only adjustable parameter in the model is D_{app} , which was varied to fit the data. D_{app} is a function of the structure of the solid and specifically its density, porosity, and tortuosity, and the specific sorbate–sorbent interactions incorporated in the conditional distribution coefficient K_d . The following section is a discussion of relevant parameter estimation.

The molecular diffusivities of cadmium and selenite ions were estimated from the Nernst–Haskell equation (39) and are given in Tables 2 and 3, respectively. Because no limiting

TABLE 3

Selenite Diffusivities in Porous Aluminas^a

	CP-5	C-33	CP-100
K_d (m ³ /g)	1.1×10^{-3}	2.8×10^{-4}	8.8×10^{-4}
R_{int} (-)	1.2×10^3	3.3×10^2	1.3×10^3
pH	6.0	5.5	6.0
D_{app} (m ² /s)	1.5×10^{-15}	5.0×10^{-14}	1.5×10^{-15}
D_{eff} (m ² /s)	1.7×10^{-12}	1.7×10^{-11}	1.9×10^{-12}
χ_e (-)	700	70	640

^a $D_{mol} = 1.20 \times 10^{-9}$ m²/s.

ionic conductance for the selenite ion was available, it was approximated by the value reported for selenate (40). The bulk density and porosity of the adsorbents were measured, and the values are reported elsewhere (36) and in Table 1. The tortuosity factor, χ , accounts for pore structure effects in a porous solid (41). The distance between two points along a tortuous path is greater than the direct distance between the two points; pore constrictions would also tend to decrease diffusion rates in a porous solid. The tortuosity factor incorporates both effects and has a value always greater than 1. At present, there is no *a priori* method for tortuosity estimation from parameters such as particle size, porosity, and pore size distribution. Tortuosities are typically estimated from diffusion experiments. Typical tortuosity values reported for catalysts range from approximately 1.5 to 10 (41). Satterfield also suggests that in the absence of diffusion measurements a tortuosity factor between 2 and 6 be used for porous solids with open interconnected pore systems.

The distribution coefficients needed in eq 2 were estimated by evaluating sorption isotherm data at four solute concentrations, using each solute and each sorbent; K_d values were evaluated at 0.5 pH unit intervals. K_d values varied over more than 1 order of magnitude for selenite adsorption over the pH range 5.5–9.5; the K_d varied by 4 orders of magnitude for cadmium adsorption on aluminas over the pH range 5–9. The K_d estimates were obtained by a least-squares fit over a solute concentration range 10^{-6} to 10^{-3} M. The resulting isotherms were not linear (see the Appendix for details of the distribution coefficient estimation method and an evaluation of the linearity of the isotherms). The nonlinearity notwithstanding, the sorption isotherms can be considered sufficiently similar, based on the similar $1/n$ values, to permit comparison by means of the K_d parameter.

Thus, it appeared warranted to use a linear isotherm instead of the Freundlich isotherm to model the rate of cadmium and selenite uptake, realizing that the distribution coefficients used were average values, not necessarily applicable to the entire range of concentrations shown. Solute concentrations, however, during a typical uptake experiment were reduced by approximately 50% during the course of the reaction (corresponding to 50% final uptake) so that errors from using these average distribution coefficients would be acceptable. Because of the similarity of interactions of either solute with the three adsorbents, respectively, use of these average distribution coefficients should allow the qualitative comparison of uptake behavior between the three sorbents even though the diffusivities determined may be inaccurate.

Modeling Results. Cadmium. Results of modeling cadmium uptake by the three porous adsorbents are shown in Figure 3. Agreement of the diffusion model with the

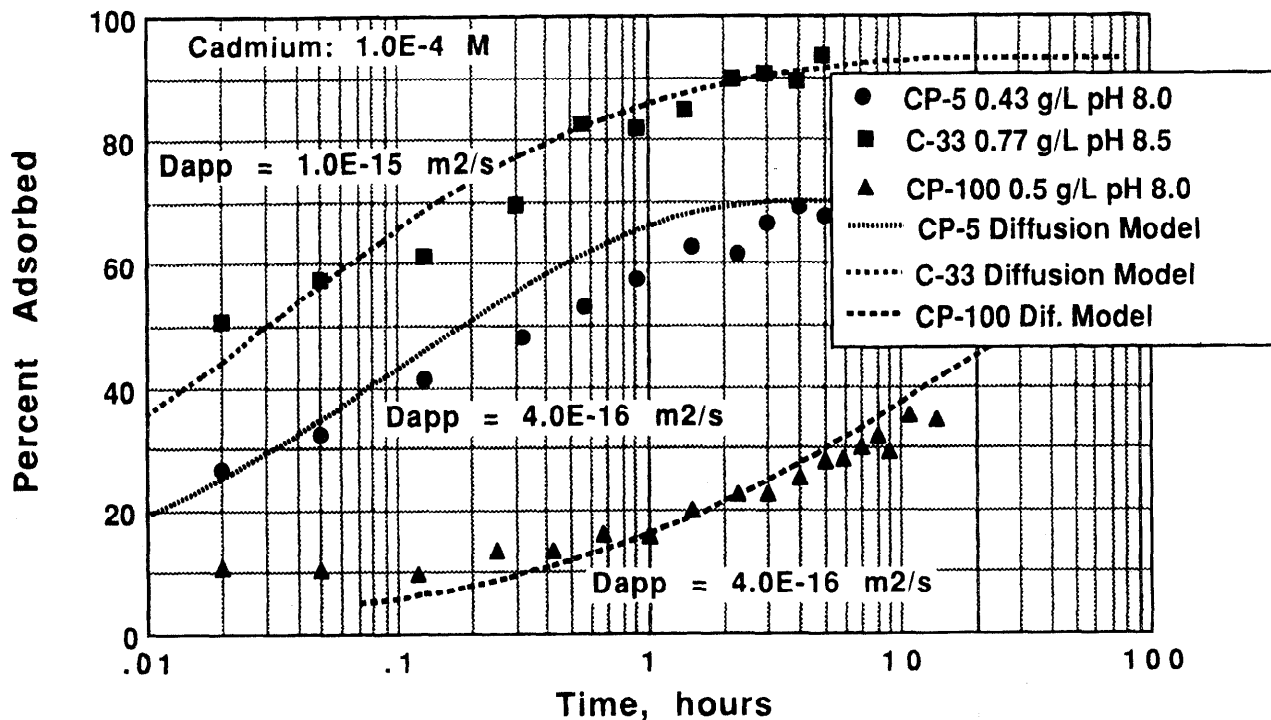


FIGURE 3. Modeling the rate of cadmium uptake by transition aluminas (CP-5, C-33, and CP-100) with the diffusion in a sphere from limited volume model.

experimental data suggests that the rate of cadmium uptake is probably controlled by intraparticle diffusion. The diffusion model slightly underestimated fractional uptake during the early phase of the experiments. The discrepancy between model and experimental data was more pronounced for CP-100 particles. Uptake enhancement during the initial phase of the experiment can be attributed to instantaneous sorption and can be explained by the increased external surface area of real particles due to surface roughness (verified by SEM (36)) compared to smooth, geometrically spherical particles. The presence of fines, with diameters substantially smaller than the volume-surface mean, could also contribute to a fast initial solute uptake.

The same apparent diffusivity ($4.0 \times 10^{-16} \text{ m}^2/\text{s}$) was used to fit rate of cadmium uptake data by CP-5 and CP-100 particles. The apparent diffusion coefficient used to model cadmium uptake by C-33 particles was higher ($1.0 \times 10^{-15} \text{ m}^2/\text{s}$). Higher diffusivities in C-33 particles are consistent with the mesopore structure of this adsorbent compared to the micropore structure of CP-5 and CP-100 (see discussion above for details). The less active surface of C-33, resulting in lower affinity for cadmium relative to the other adsorbents, is reflected in lower retardation factors for cadmium sorption on C-33 and therefore higher apparent diffusivities. A discussion of structure-activity relationships in aluminas was presented by Wefers and Misra (37) and summarized by Papelis (36). The reported internal retardation factor for C-33 is only similar to the retardation factors for CP-5 and CP-100 because the experiments with C-33 were conducted at higher pH (8.5), and as was already mentioned, distribution coefficients are a strong function of pH for inorganic ion sorption.

A comparison of apparent diffusivities and the estimated bulk aqueous molecular diffusivity for the cadmium ion (Table 2) shows that the experimentally determined apparent diffusivities were orders of magnitude lower than

bulk diffusivities. Even when internal retardation is taken into account, the resulting effective diffusivity, D_{eff} , is still substantially lower than the bulk aqueous diffusivity (Table 2). The difference between the two diffusivities can be assigned to the tortuosity factor, χ (eq 3), which essentially serves as a fitting parameter, χ_e , the effective tortuosity.

As was mentioned above, the tortuosity incorporates the effects of longer (tortuous) diffusion paths and pore constrictions, dead ends, or other steric hindrance, especially in micropores, on solute diffusion. A comparison of calculated effective tortuosities (shown in Table 2) and tortuosity values reported in the literature for catalysts (between 2 and 10) suggests the presence of strong steric hindrance effects in these adsorbents. Such steric hindrance is plausible, at least in the case of CP-5 and CP-100, the microporous adsorbents. Although the effective tortuosities are of the same order of magnitude for all three adsorbents, χ_e for C-33 is slightly lower than for CP-5 or CP-100 (95 vs 200 or 300), as expected from the pore structure characteristics of the three adsorbents (36).

Selenite. Results of modeling selenite uptake by the three aluminas are shown in Figure 4. The diffusion model adequately represents selenite uptake by the three solids as a function of time. Instantaneous sorption was not significant in the case of selenite sorption. The same diffusivity ($1.5 \times 10^{-15} \text{ m}^2/\text{s}$) was used for CP-5 and CP-100 adsorbents; a higher value for the diffusivity ($5.0 \times 10^{-14} \text{ m}^2/\text{s}$) was necessary to model uptake by C-33 adsorbents for the same reasons discussed with respect to cadmium uptake.

The selenite modeling results are presented in Table 3. There is substantial difference in the K_d values for the three solids, with the more crystalline material (C-33) having the lower K_d . The lower K_d , or lower affinity of selenite for the C-33 surface, reflects the lower reactivity of the C-33 surface compared to those of CP-5 and CP-100. CP-5 and CP-100 are more disordered and therefore more reactive phases

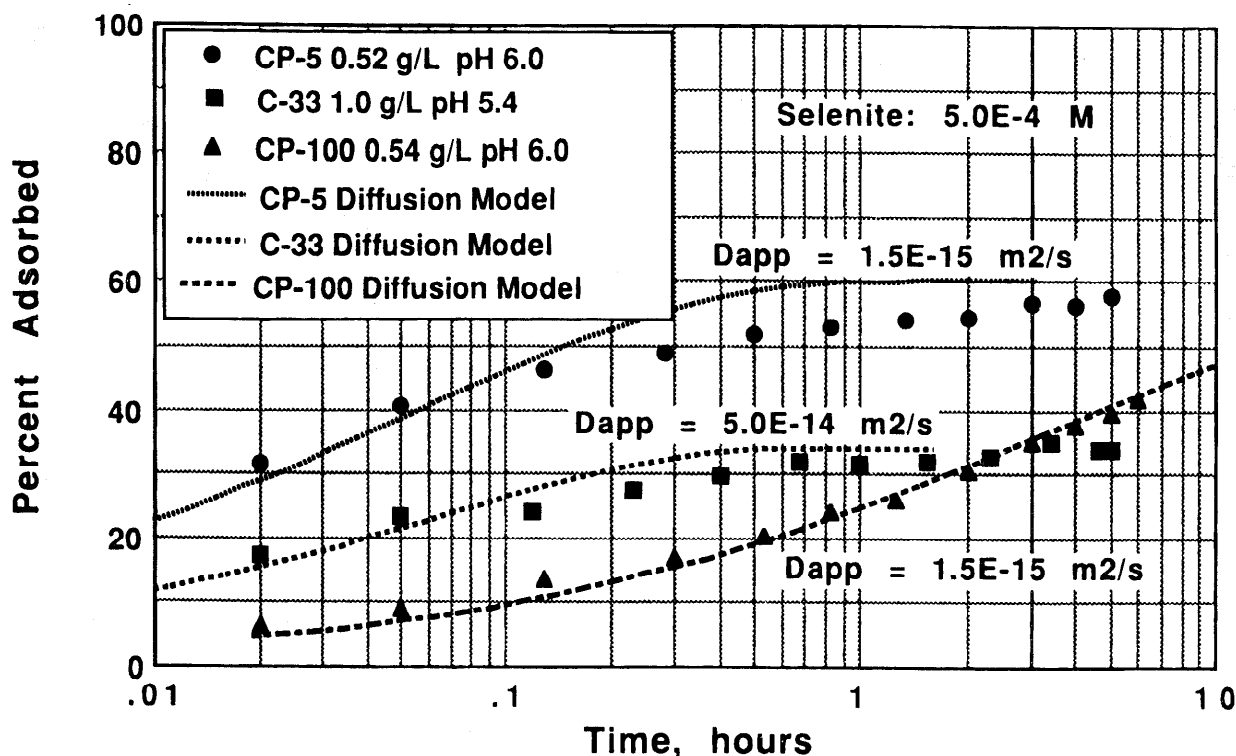


FIGURE 4. Modeling the rate of selenite uptake by transition aluminas (CP-5, C-33, and CP-100) with the diffusion in a sphere from limited volume model.

than C-33 (36). Indirectly then, the higher reactivity of the surface results in lower apparent diffusion coefficients. From Table 3, it can also be seen that the effective tortuosities were not the same for all three solids. The effective tortuosities were essentially constant for the two similar solids (CP-5 and CP-100), but χ_e was lower for C-33 by an order of magnitude.

Comparison of Cadmium and Selenite. By comparing the cadmium and selenite modeling results, several important differences can be noted. K_d values for selenite sorption were a stronger function of the solid than K_d values for cadmium sorption at the pH value of the experiments shown. The calculated values of D_{app} were therefore expected to be a stronger function of the solid for selenite adsorption than for cadmium adsorption owing to the retardation effect (eq 2); this anticipated difference is confirmed by comparing the results in Tables 2 and 3. The larger variation of K_d as a function of solid for selenite sorption at low pH is caused by the lower capacity of C-33 for selenite at conditions near monolayer coverage (36). It is reasonable to assume that differences in surface reactivity may be more evident under conditions of higher surface coverage. It should be remembered that the selenite concentration was 5×10^{-4} M. In the case of cadmium, the highest concentration that did not result in the formation of a precipitate was 1×10^{-4} M. Selenite surface coverages were, therefore, higher than cadmium surface coverages.

For both cadmium and selenite, the effective tortuosities were as expected, larger for the microporous solids (CP-5 and CP-100) than for the mesoporous solid (C-33). The difference between microporous and mesoporous solids, however, was more pronounced in the case of selenite. Although χ_e was approximately the same for cadmium and selenite diffusion in C-33, the effective tortuosity was approximately two to three times larger for selenite

compared to cadmium in the microporous solids. It is possible that microporosity is more important in the case of selenite adsorption compared to cadmium adsorption. Steric hindrance effects may be more critical for selenite than for cadmium because of the size differences between the smaller cadmium cation and the bigger selenite anion.

On the basis of spectroscopic evidence (42), it was determined that the Cd-O distance in the fully hydrated, octahedrally coordinated cadmium cation is 2.33 Å. This is the distance between the central metal cation and the oxygens of the surrounding first hydration sphere of water molecules, resulting in a diameter of approximately 4.7 Å for the fully hydrated cadmium cation (including its first hydration sphere). Similarly, spectroscopic evidence (42, 43) has confirmed the Se-O distance in the selenite ion as 1.69 Å, resulting in a diameter of the bare selenite anion of approximately 3.4 Å.

It is more difficult to estimate the size of the fully hydrated anion. On the basis of spectroscopic data analysis of selenite sorption on goethite (43), however, it was estimated that the second coordination shell (corresponding to the Se-Fe distance) was 3.38 Å. In the case of selenate ion adsorption on goethite (43), where the primary hydration sphere was assumed to be retained by the selenate ion upon adsorption, the Se-Fe distance could not be determined, suggesting that it was probably larger than 4-6 Å. It is therefore not unreasonable to assume a diameter for the fully hydrated selenite anion (including its first hydration sphere) of approximately 6-7 Å, i.e., of the same order of magnitude as the finer pores in the microporous CP-5 and CP-100.

Finally, the observed difference in behavior between cadmium and selenite diffusion could be a function of the pH at which the experiments were conducted. A pH of at least 8 was required for significant uptake of 0.1 mM cadmium, whereas lower pH (below 6-7) was required for

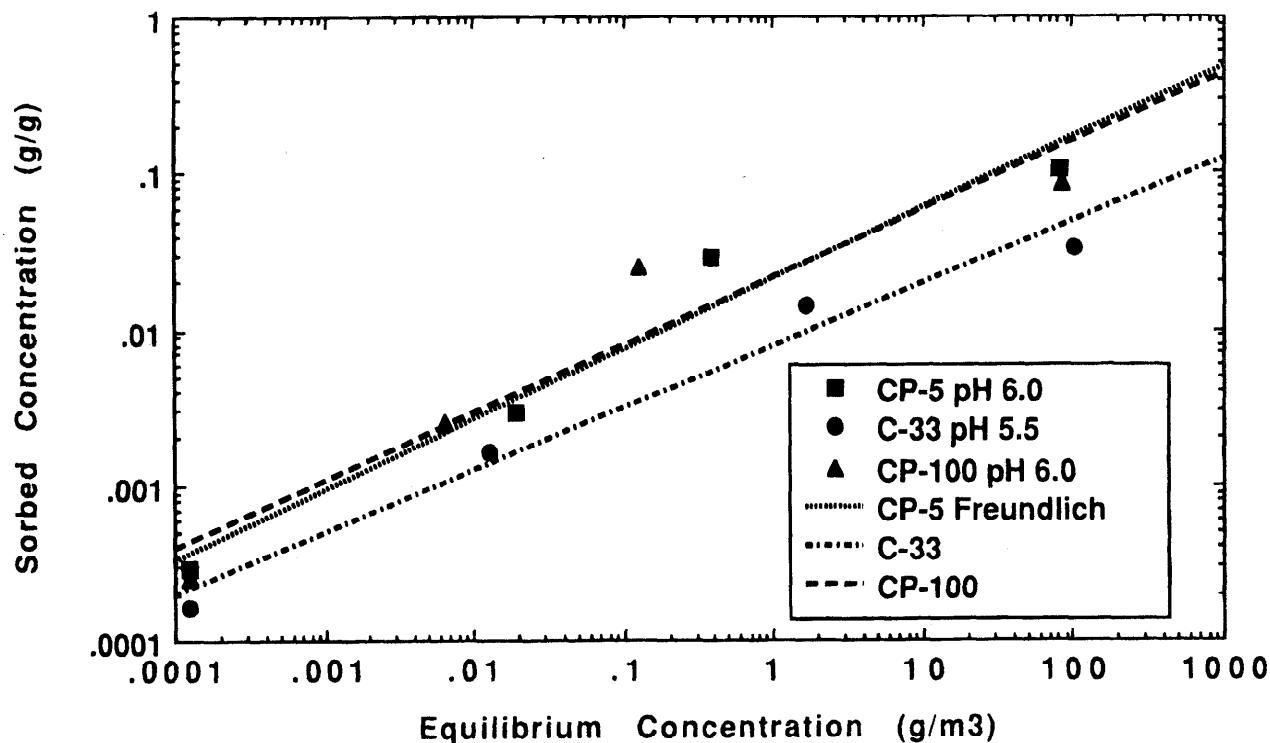


FIGURE 5. Fit of equilibrium isotherms for sorption of selenite on CP-5, C-33, and CP-100 transition aluminas by the Freundlich isotherm.

significant uptake of selenite. The higher pH value (8–8.5) corresponds approximately to the pH_{PZC} of these aluminas; the surface of the aluminas will have almost no charge at conditions favoring cadmium adsorption, and there will be an almost even distribution of co-ions and counterions in the diffuse layer. At lower pH, the surface is positively charged, and counterions (nitrate ions) predominate in the diffuse layer. Adsorption of cadmium therefore requires little counter-diffusion of cadmium and sodium ions, whereas adsorption of selenite requires a higher counter-diffusion rate of selenite and nitrate ions. The hypothesis that counter-diffusion limits diffusion rates in micropores more than in mesopores would explain the differences in effective tortuosities between the mesoporous adsorbent (C-33) and the micropore-containing adsorbents (CP-5 and CP-100). A significant portion of the total surface area of CP-5 and CP-100 particles was associated with micropores. Note also that the effective tortuosity for selenite adsorption on C-33, where microporosity was absent, was similar to the effective tortuosity estimated for cadmium adsorption.

Conclusions

Rate experiments showed distinct differences in the uptake of selenite and cadmium by the three transition aluminas studied. Ion uptake was considerably faster by CP-5 and C-33 aluminas. Approximately 3 h was required for equilibrium for CP-5 and C-33 whereas several days was required for the larger CP-100 particles. These differences between CP-5 and CP-100 are largely based on particle size differences, because these oxides had otherwise similar characteristics. Differences in the uptake behavior of C-33 and the other two adsorbents were related to their different physical and chemical characteristics, including pore structure (microporosity or absence thereof), and different crystal structure resulting in surfaces of different activity and therefore different affinity for cadmium and selenite.

The diffusion model was in fair agreement with the data, suggesting that the rate of cadmium and selenite uptake

by porous aluminas is controlled by mass transfer. For cadmium uptake, the apparent diffusivities ranged from $4.0 \times 10^{-16} \text{ m}^2/\text{s}$ for CP-5 and CP-100 to $1.0 \times 10^{-15} \text{ m}^2/\text{s}$ for C-33. Selenite diffusivities ranged from $1.5 \times 10^{-15} \text{ m}^2/\text{s}$ for CP-5 and CP-100 to $5.0 \times 10^{-14} \text{ m}^2/\text{s}$ for C-33.

Differences in cadmium diffusivities between the adsorbents can be accounted for by their different pore structure (affecting tortuosity) and different surface reactivity (reflected in different distribution coefficients). The resulting effective tortuosities were similar. The spread in effective tortuosities was more significant for selenite adsorption. Possible explanations hinge on the more important role that microporosity may have on selenite adsorption. First, steric hindrance effects may be more important to the diffusion of the bigger selenite oxyanion as opposed to the smaller cadmium cation. Second, at the pH of selenite adsorption, which is further away from the pH_{PZC} than the pH of cadmium adsorption, a greater imbalance between co-ions and counterions in the diffuse layer may be controlling the diffusion rate of selenite in micropores and thus lead to substantial rate of uptake differences between the micro- and non-microporous solids, which is not accounted for by parameters such as retardation and tortuosity.

Appendix: Estimation of Distribution Coefficients

The distribution coefficients reported in Tables 2 and 3 were estimated from equilibrium isotherm data presented elsewhere (36), obtained by equilibrating for a period of 1 week. Four total sorbate concentrations (ranging from 1.0×10^{-6} to $1.0 \times 10^{-3} \text{ M}$) were used for each sorbent-sorbate system. Because of the strong dependence of the distribution coefficients on pH, the distribution coefficients were evaluated at 0.5 pH unit intervals. Cadmium distribution coefficients for pH values above 7.5 were based on three points only, because of the formation of a cadmium precipitate at higher pH values and a total cadmium concentration $1.0 \times 10^{-3} \text{ M}$.

TABLE 4

Distribution Coefficients from Cadmium Equilibrium Sorption Isotherms

sorbent	pH	K_d (m ³ /g)	intercept (g/g)	r^2
CP-5	8.0	1.02×10^{-2}	8.61×10^{-4}	0.997
C-33	8.5	1.05×10^{-2}	6.27×10^{-4}	0.995
CP-100	8.0	1.10×10^{-2}	6.38×10^{-4}	0.998

TABLE 5

Distribution Coefficients from Selenite Equilibrium Sorption Isotherms

sorbent	pH	K_d (m ³ /g)	intercept (g/g)	r^2
CP-5	6.0	1.13×10^{-3}	1.04×10^{-2}	0.931
C-33	5.5	2.75×10^{-4}	5.18×10^{-3}	0.836
CP-100	6.0	8.76×10^{-4}	9.26×10^{-3}	0.917

TABLE 6

Freundlich Isotherm Parameters from Cadmium Equilibrium Sorption Isotherms

sorbent	pH	K_F (g/g)/(g/m ³) ^{1/n}	1/n (-)	r^2
CP-5	8.0	1.1×10^{-2}	0.43	0.979
C-33	8.5	1.2×10^{-2}	0.59	1.000
CP-100	8.0	1.1×10^{-2}	0.54	0.988

TABLE 7

Freundlich Isotherm Parameters from Selenite Equilibrium Sorption Isotherms

sorbent	pH	K_F (g/g)/(g/m ³) ^{1/n}	1/n	r^2
CP-5	6.0	2.1×10^{-2}	0.45	0.980
C-33	5.5	7.6×10^{-3}	0.40	0.987
CP-100	6.0	2.1×10^{-2}	0.43	0.955

The K_d values, the intercepts, and the correlation coefficients, r^2 , obtained from cadmium and selenite sorption isotherms are listed in Tables 4 and 5, respectively. When plotted on a logarithmic scale (Figure 5), it can be seen that the isotherms were not linear. The sorption data were therefore fitted by the Freundlich isotherm, and fits are also shown in Figure 5 for selenite.

The Freundlich isotherm parameters, K_F and $1/n$, are shown in Tables 6 and 7. It can be seen from Tables 6 and 7 that the Freundlich isotherm exponents were similar for all adsorbents for both cadmium and selenite (ranging from 0.43 to 0.59 for cadmium sorption and from 0.40 to 0.45 for selenite sorption) under these specific experimental conditions.

Acknowledgments

Financial support for this project was provided by the U.S. Environmental Protection Agency Western Region Hazardous Substance Research Center through EPA Grant R-815738. This article has not been reviewed by the U.S. Environmental Protection Agency and, therefore, does not necessarily reflect the views of this agency. We thank G. P. Curtis for the FORTRAN implementation of the solution to the diffusion equation. Helpful discussions with D. B. Kent and the thoughtful comments of two anonymous reviewers are also acknowledged.

Literature Cited

- Ball, W. P.; Roberts, P. V. *Environ. Sci. Technol.* **1991**, *25*, 1237-1249.
- Bahr, J. M. *J. Contam. Hydrol.* **1989**, *4*, 205-222.
- Brusseau, M. L.; Rao, P. S. C.; Jessup, R. E.; Davidson, J. M. *J. Contam. Hydrol.* **1989**, *4*, 223-240.
- Brusseau, M. L.; Jessup, R. E.; Rao, P. S. C. *Environ. Sci. Technol.* **1990**, *24*, 727-735.
- Brusseau, M. L.; Jessup, R. E.; Rao, P. S. C. *Environ. Sci. Technol.* **1991**, *25*, 134-142.
- Goltz, M. N.; Roberts, P. V. *J. Contam. Hydrol.* **1988**, *3*, 37-63.
- Boyd, G. E.; Adamson, A. W.; Myers, L. S., Jr. *J. Am. Chem. Soc.* **1947**, *69*, 2836-2848.
- Boyd, G. E.; Myers, L. S., Jr.; Adamson, A. W. *J. Am. Chem. Soc.* **1947**, *69*, 2849-2859.
- Ogwada, R. A.; Sparks, D. L. *Soil Sci. Soc. Am. J.* **1986**, *50*, 1158-1162.
- Ogwada, R. A.; Sparks, D. L. *Soil Sci. Soc. Am. J.* **1986**, *50*, 1162-1166.
- Davis, J. A.; Hayes, K. F. In *Geochemical Processes at Mineral Surfaces*; Davis, J. A., Hayes, K. F., Eds.; ACS Symposium Series 323; American Chemical Society: Washington, DC, 1986; pp 2-18.
- Hayes, K. F. Ph.D. Dissertation, Stanford University, Stanford, CA, 1987.
- Anderson, M. A.; Rubin, A. J., Eds. *Adsorption of Inorganics at Solid-Liquid Interfaces*; Ann Arbor Science: Ann Arbor, MI, 1981; p 357.
- Nyffeler, U. P.; Li, Y. H.; Santschi, P. H. *Geochim. Cosmochim. Acta* **1984**, *48*, 1513-1522.
- Theis, T. L.; Iyer, T. L.; Kaul, L. W. *Environ. Sci. Technol.* **1988**, *22*, 1013-1017.
- Stumm, W. *Chemistry of the Solid-Water Interface*; John Wiley & Sons: New York, 1992; p 428.
- Hachiya, K.; Sasaki, M.; Saruta, Y.; Mikami, N.; Yasunaga, T. *J. Phys. Chem.* **1984**, *88*, 23-27.
- Hachiya, K.; Sasaki, M.; Ikeda, T.; Mikami, N.; Yasunaga, T. *J. Phys. Chem.* **1984**, *88*, 27-31.
- Hayes, K. F.; Leckie, J. O. In *Geochemical Processes at Mineral Surfaces*; Davis, J. A., Hayes, K. F., Eds.; ACS Symposium Series 323; American Chemical Society: Washington, DC, 1986; pp 114-141.
- Mikami, N.; Sasaki, M.; Kikuchi, T.; Yasunaga, T. *J. Phys. Chem.* **1983**, *87*, 5245-5248.
- Yasunaga, T.; Ikeda, T. In *Geochemical Processes at Mineral Surfaces*; Davis, J. A., Hayes, K. F., Eds.; ACS Symposium Series 323; American Chemical Society: Washington, DC, 1986; pp 230-253.
- Zhang, P. C.; Sparks, D. L. *Soil Sci. Soc. Am. J.* **1990**, *54*, 1266-1273.
- Zhang, P. C.; Sparks, D. L. *Environ. Sci. Technol.* **1990**, *24*, 1848-1856.
- Farley, K. J.; Dzombak, D. A.; Morel, F. M. M. *J. Colloid Interface Sci.* **1985**, *106*, 226-242.
- Dzombak, D. A.; Morel, F. M. M. *J. Colloid Interface Sci.* **1986**, *112*, 588-598.
- Fuller, C. C.; Davis, J. A.; Waychunas, G. A.; Rea, B. A. *Geochim. Cosmochim. Acta* **1993**, *57*, 2271-2282.
- Curtis, G. P.; Reinhard, M.; Roberts, P. V. In *Geochemical Processes at Mineral Surfaces*; Davis, J. A., Hayes, K. F., Eds.; ACS Symposium Series 323; American Chemical Society: Washington, DC, 1986; p 683.
- Leckie, J. O.; Tripathi, V. S. *Effect of geochemical parameters on the distribution coefficient K_d* ; Presented at Heavy Metals in the Environment; Athens, Greece, Sept 1985; CEP Consultants Ltd: Edinburgh, UK, 1985; Vol 2, pp 369-371.
- Reynolds, W. D.; Gillham, R. W.; Cherry, J. A. *Can. Geotech. J.* **1982**, *19*, 92-103.
- Nakamura, S.; Mori, S.; Yoshimuta, H.; Ito, Y.; Kanno, M. *Sep. Sci. Technol.* **1988**, *23*, 731-743.
- Ohnuki, T.; Takebe, S.; Yamamoto, T. *J. Nucl. Sci. Technol.* **1989**, *28*, 795-804.
- Ooi, K.; Ashida, K.; Katoh, S.; Sugasaki, K. *J. Nucl. Sci. Technol.* **1987**, *24*, 315-322.
- Kent, D. B.; Tripathi, V. S.; Ball, N. B.; Leckie, J. O. *Surface-complexation modeling of radionuclide adsorption in sub-surface environments*; Technical Report 294; Department of Civil Engineering, Stanford University, Stanford, CA, 1986.
- Wood, W. W.; Kraemer, T. F.; Hearn, P. P., Jr. *Science* **1990**, *247*, 1569-1572.
- Gregg, S. J.; Sing, K. S. W. *Adsorption, Surface Area and Porosity*; Academic Press Inc.: London, 1982; p 303.

- (36) Papelis, C. Ph.D. Dissertation, Stanford University, Stanford, CA, 1992.
- (37) Wefers, K.; Misra, C. *Oxides and Hydroxides of Aluminum*; Alcoa Technical Paper 19, Revised; Aluminum Company of America: Pittsburgh, 1987.
- (38) Crank, J. *The Mathematics of Diffusion*; Oxford University Press: Oxford, 1975; p 414.
- (39) Reid, R. C.; Prausnitz, J. M.; Sherwood, T. K. *The Properties of Gases and Liquids*; McGraw-Hill: New York, 1977; p 688.
- (40) Weast, R. C., Ed. *Handbook of Chemistry and Physics*, 71st ed.; CRC Press, Inc.: Boca Raton, FL, 1990.
- (41) Satterfield, C. N. *Mass Transfer in Heterogeneous Catalysis*; R. E. Krieger Publishing Co., Inc.: Malabar, FL, 1981; p 267.
- (42) Papelis, C.; Brown, G. E., Jr.; Parks, G. A.; Leckie, J. O. Submitted for publication to *Langmuir* 1994.
- (43) Hayes, K. F.; Roc, A. L.; Brown, G. E., Jr.; Hodgson, K. O.; Leckie, J. O.; Parks, G. A. *Science* **1987**, 238, 783.

Received for review August 23, 1994. Revised manuscript received December 14, 1994. Accepted December 21, 1994.*

ES940537A

* Abstract published in *Advance ACS Abstracts*, February 1, 1995.